iJRASET
International Journal For Research in Applied Science and Engineering Technology

# INTERNATIONAL JOURNAL FOR RESEARCH

IN APPLIED SCIENCE & ENGINEERING TECHNOLOGY

**Volume:** 7 **Issue:** V **Month of publication:** May 2019

**DOI:** https://doi.org/10.22214/ijraset.2019.5600

www.ijraset.com

Call: 08813907089 | E-mail ID: ijraset@gmail.com

International Journal for Research in Applied Science & Engineering Technology (IJRASET)
*ISSN: 2321-9653; IC Value: 45.98; SJ Impact Factor: 7.177*
*Volume 7 Issue V, May 2019- Available at www.ijraset.com*

# Synthesis of MWCNTs/x%$TiO_2$ nanocomposites via Evaporation Method for Decontamination of some Local Textile Dyes

Walied A. A. Mohamed[1], Badr A. El-sayed[2], Hoda R. Galal[3], H. M. H. Abd El-Bary[4], Mahmoud A. M. Ahmed[5]
[1, 3]*Ass. Dr. Professor,* [2,4]*Professor and* [5]*PHD Student*
[1, 3]*Department of Inorganic Chemistry, National Research Centre, Cairo, Egypt.*
[2, 4, 5]*Department of Chemistry, Faculty of Science, Al-Azhar University, Cairo, Egypt.*

***Abstract:*** ***Multi-walled carbon nanotubes/titanium dioxide nanocomposites MWCNTs/x%$TiO_2$ with different weight ratios of $TiO_2$ (x = 3, 6 and 10%) have been synthesized using a simple modified evaporation method. The structure of the synthesized nanocomposite photocatalysts were characterized using XRD, SEM, $N_2$ adsorption-desorption and diffused reflectance UV-Vis spectroscopic techniques. The photocatalytic activity of the synthesized photocatalysts toward decontamination of two local textile dyes (Dianix Blue and Vat Green 1 Dyes) as an industrial organic pollutants commonly used in dyeing factories in Egypt. Moreover, the suggested possible mechanism of the photodegradation processes was studied. Also optical band gap was estimated by Kubelka-Munk equation for MWCNTs and MWCNTs/x%$TiO_2$ (x = 3, 6 and 10%) giving rises values 3.51, 2.89, 2.80, 2.69 eV respectively. The photodegradation of the two textile dyes after complete degradation were measured using chemical oxygen demand processes.***

***Keywords: MWCNTs/x%$TiO_2$ Nanocomposites, Dipping Method, Photocatalytic Activity, Dianix Blue Dye, Vat Green 1 Dye.***

## I. INTRODUCTION

Carbon nanotubes (CNTs) have attracted a lot of attention as a result of their mechanical properties, novel 1D (nanotube) character, unique properties and promising potential applications [1-7]. The uniformity in diameter, the dearth of purity, chirality and alignment has hindered searching of the intrinsic properties such as electronic, mechanical, sorption properties of CNTs in addition to their applications in novel electronic systems [8-12]. In last decades, various researches have been devoted to study the structure of CNTs and their high level surface area, stability toward electrochemical processes, thermal and electrical properties. Due to their exceptional properties, CNTs were introduced as applicants for excellent environmentally friendly uses such as filtration in separation techniques. CNTs have been used in removing hazardous pollutants from wastewater in industrial field such as leather and textile [13]. Due to its effectiveness, ideally producing nontoxic end products and easy operation, photocatalysis has been commonly used as a technique for the removing of industrial hazardous pollutants. $TiO_2$ (anatase) as a semiconductor with direct bandgap of 3.18 eV (wavelength, lower than 388 nm), has been used as an active photocatalyst. The quick recombination problem of photogenerated charge carriers (electron-hole pairs), alters photocatalytic efficiency and reduces the quantum efficiency of the photocatalytic process. Therefore, in recent years, many authors have been designed and developed nanocomposites including $TiO_2$ to avoid this problem and the pairing effect of MWCNTs with $TiO_2$ has been presented to provide a synergistic effect which can enhance the overall reaction of the dyes photodegradation [14-20], also $TiO_2$ can combined with other materials to like multi-nano walled carbon nanotubes to obtain good performance as photocatalyst [16] . The prepared nanocomposites were evaluated for the photodegradation of the Dianix Blue and Vat Green 1 Dyes under Sunlight, UV and Xenon lamps as well as the degree of complete mineralization of the two dyes were assessed.

## II. EXPERIMENTAL

### *A. Materials*

Dianix Blue Dye (4,8-diamino-1,5-dihydroxy-2-(4-hydroxyphenyl)-4a,9a-dihydroanthracene-9,10-dione) molecular weight 362.34 and the molecular formula $C_{20}H_{14}N_2O_5$ and Vat Green 1 Dye (Anthra[9,1,2-cde] benzo[rst]pentaphene-5,10- dione, 16,17-dimethoxy) with molecular weight 516.54 and the molecular formula $C_{36}H_{20}O_4$, both of these dye used in dyeing process in Egyptian Spinning & Weaving Company, Cairo, Egypt. Sulphuric acid ($H_2SO_4$) 3M, nitric acid ($HNO_3$) 2M, $TiO_2$ (Degussa P25) and deionized water. All purchased from SCRC, China and Merck and all chemical reagents were of analytical grade and used without further purification.

*B. Measurements Techniques*

1) *Scanning Electron Microscopy (SEM):* Characterizations of the surface morphology of MWCNTs and MWCNTs/x%$TiO_2$ nanocomposites were observed through Scanning Electron Microscopy (SEM) performed using Philips XL-30 SEM analyzer (JEOL – JSM – T330 A) with an acceleration voltage 30 KV instrument.
2) *X-ray Diffraction (XRD):* XRD patterns were recorded by Philips Holland. Xpert MPD model using Cu-Kα target. (Cu Kα radiation = 0.154 nm, 50 kV, 40 mA; data recorded at a 0.017□ step size, 100 s/step).
3) *UV-Vis Spectrophotometers:* UV-Vis spectroscopy was conducted to monitor the concentration of some organics in liquid phase, which were being oxidized through photocatalytic degradation. The concentration of the investigated dyes after photodegradation was analyzed using a UV-Vis spectrophotometer (Schimadzu)
4) *Chemical Oxygen Demand (COD):* The chemical oxygen demand COD is based on the chemical decomposition of compounds, dissolved or suspended in water by using COD Hanna Professional Instrument.
5) *Photochemical Reactors:* The experimental setup was employed for the photocatalytic studies by using both of photoreactors 80-W UV-lamp and 50-W Xe-lamp (Eng. Co., Ltd., Egypt). Sunlight intensity for our photodegradation processes was nearly about 3.4 lux for UV light and 1009 lux for visible light, was measured by (Lx-102 light meter).

*C. Synthesis of MWCNTs and MWCNTs/x%TiO2 nanocomposites*

1) *Synthesis of MWCNTs:* High purity MWCNTs were synthesized according to the literatures previously reported with some modification [21]. In the present paper, MWCNTs were prepared by CVD method. The reactants were vaporized into a hydrogen/argon atmosphere at 720 □. The MWCNTs as well as residual iron catalyst particles were removed by annealing the as-grown MWCNTs in argon at 1750 □ for 5 h. The production yield, which indicates the yield of multi-walled carbon nanotubes in the converted carbon, reaches 95%. One gram of MWCNTs was dispersed in the mixed acids consisting of 30 mL of concentrated $H_2SO_4$ and 10 mL of concentrated $HNO_3$ with ultrasonication for 7 h to activate the surfaces, then washing and drying at 100 □.
2) *Synthesis of MWCNTs/x%TiO2 nanocomposites:* MWCNTs/x%$TiO_2$ nanocomposites were prepared by a simple modified evaporation method. MWCNTs were dispersed in water in a 200-mL beaker and sonicated for 30 min. $TiO_2$ (Degussa P25) powder, Anatase and Rutile mixture (78%:22%) was added to MWCNTs suspension at different ratios of 1, 3, 6 and 10% (MWNT:$TiO_2$) during sonication. The suspension was filtered by using a vacuum evaporator to accelerate the water evaporation rate at 45 □. Then, the MWCNTs/x%$TiO_2$ composite was dried at 105 □ for 24 h to avoid any probability of physicochemical change in the carbon materials may occurs in the presence of oxygen at higher temperatures.

*D. Photocatalytic Processes*

The photocatalytic processes of Dianix blue and Vat green 1 dyes were carried out using advanced oxidation processes (AOP's) with different light sources such as Sunlight, UV and Xenon irradiation without photocatalysts, and With different amount of photocatalysts MWCNTs, MWCNTs/3%$TiO_2$-MWCNTs/6%$TiO_2$-MWCNTs/10%$TiO_2$ nanocomposites with the different illumination sources for various irradiation times to identify the most suitable and economical process for complete decolourization and substantial mineralization of the two textile dyes. The effect of various experimental parameters such as irradiation time, photocatalyst concentrations, substrate concentrations of the dyes were carried out to arrive the optimized experimental conditions. To study the effect of substrate concentration, the photocatalytic degradation experiments were carried out at the optimized photocatalyst concentrations. For this the substrate concentrations, i.e. concentrations of Dianix Blue dye were varied from $2.8\times10^{-5}$ M to $2\times10^{-5}$ M and concentrations of Vat Green 1 dye were varied from $2.2\times10^{-5}$ M to $1.6\times10^{-5}$ M. The photodegradation experiments were carried out in the photoreactors in which 100 ml of both of the two textile dye solutions were taken and the photocatalyst concentrations were 0.1g/100 ml for all photocatalytic processes. The solutions were agitated with the help of aeration pump and magnetic stirrer. On the other hand study of the effect of irradiation time of photocatalytic degradation experiments were carried up to 7 h. The effect of the catalyst concentration was studied by varying the amounts of MWCNTs/3%$TiO_2$, MWCNTs/6%$TiO_2$ and MWCNTs/10%$TiO_2$ nanocomposites with the irradiation with Sunlight, UV and Xenon lamps. For each experiment, the aliquot was taken out after a certain time with the help of the Pipet, which was then filtered and analyzed for its concentration with Schimadzu UV-Visible spectrophotometer to study the decolourization and degradation progress. The experimental setups were employed for the photocatalytic studies by using both of photoreactors 80-W UV-lamp and 50-W Xe-lamp (Eng. Co., Ltd., Egypt) and sunlight intensity of photodegradation processes was nearly about 3.4 lux for UV light and 1009 lux for visible light measured by (Lx-102 light meter). The concentration of the investigated dyes after photodegradation were

analyzed by using a UV-Vis spectrophotometer (Schimadzu) by measuring the change in their maximum absorbance values at 625 nm for Dianix Blue dye and at 626 nm for Vat Green 1 dye. Also the mineralization of the dyes was confirmed by COD analysis.

## III.RESULTS AND DISCUSSION

### A. *Characterizations and Measurements*

1) *XRD patterns of MWCNTs and MWCNTs/x%$TiO_2$ Nanocomposites:* The characteristic peaks around 25.7° and 41.9° appeared in XRD patterns as shown in (Figure - 1 (a)) were correspond to the (002) and (100) planes respectively reflected on the prepared MWCNTs. The obtained results were resemble to the previous works [19, 22]. On the other hand the characteristic peaks observed in XRD patterns for MWCNTs/x%$TiO_2$ nanocomposites as shown in (Figure - 1 (b), (c) and (d)) located at 2Θ = 25.17°,36.48°,48.84°,54.66° and 62.37°, correspond the (101), (004), (200), (211) and (204) planes respectively reflected on the prepared MWCNTs/x%$TiO_2$ nanocomposites. The shifts of the peaks is as a result for the trapping of the electrons at the active sites of the nanocomposites, which results in hindering electron-hole pair recombination [23, 24].

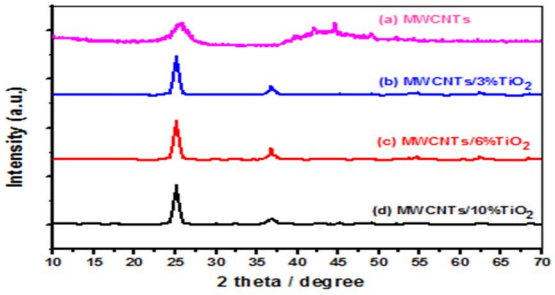


Fig.-1 Shows XRD patterns of the prepared MWCNTs and different MWCNTs/$TiO_2$ nanocomposites.

2) *Morphological study of MWCNTs and MWCNTs/x%$TiO_2$ nanocomposites surfaces:* The surface morphologies of the prepared MWCNTs and MWCNTs/x%$TiO_2$ nanocomposites were measured by Scanning Electron Microscopy (SEM) as shown in (Figure - 2). It explains the different morphology between the prepared samples and indicates that the MWCNTs/x%$TiO_2$ nanocomposites present a homogeneous distribution of $TiO_2$ on the MWCNTs surface and less agglomeration of $TiO_2$ particles on MWCNTs surface, suggesting a strong interphase structure effect between $TiO_2$ and MWCNTs. So as to increase the surface area of the nanocomposites, so it was considered that MWCNTs/x%$TiO_2$ nanocomposites could perform much more activity and show a high photocatalytic activity. The patterns demonstrate the highly crystalline nature of the nanocomposites. It can be clearly seen that the surfaces of $TiO_2$ modified with MWCNTs are rough and little $TiO_2$ particles were dispersed on the MWCNTs enhancing the $TiO_2$ in photocatalytic activity of the nanocomposite.

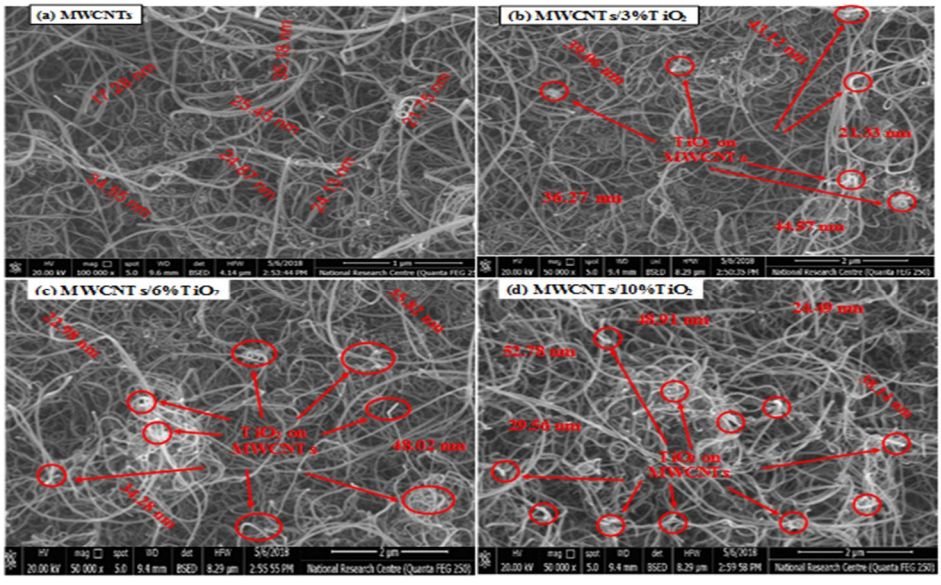


Fig.-2 Shows SEM images of the prepared MWCNTs and different MWCNTs/$TiO_2$ nanocomposites.

3) *The optical band gaps of MWCNTs and MWCNTs/x%$TiO_2$ Nanocomposites:* The band gap energy of the prepared MWCNTs and its composites was determined using UV-Vis diffuse reflectance spectroscopy in Kubelka-Munk units. The nanocomposite material can absorb almost the entire range of visible region, which is caused by the addition of MWCNTs. For a semiconductor materials, the investigation of optical absorption is considered as an appropriate method for calculation of the optical band gaps and determining the kinds of transitions. The diffuse reflectance (R) converted into equivalent absorption coefficient F (R) using Kubelka–Munk equation (equation 1) [25], it may be written as in (equation 2):

$$F(R) = \frac{(1-R)^2}{2R} \quad (1)$$

$$\left(\frac{(1-R)^2}{2R}.E\right)^{1/n} = (F(R).E)^{1/n} \quad (2)$$

Where (E) energy of light, n is an inter number = ½ and 2 for direct and indirect allowed transitions, respectively, which characterizes the transition process, thus giving direct and indirect bandgaps. The band gap for the photocatalysts may be determined from the plot of $(F(R).E)^{1/n}$ versus energy of light (E) measured in eV, from the intersection of the tangent via inflection point in absorption band and the photon energy axis. Optical energy band gap was calculated using Tauc relation (see equation 3):

$$(\alpha h\nu)^{1/n} = B(h\nu - E_g) \quad (3)$$

Which may be written as the equation (4):

$$(F(R).E)^{1/n} = B(h\nu - E_g) \quad (4)$$

where n= ½ and 2 for direct and indirect transitions, respectively, α is (absorption coefficient), h is (a Planck constant), ν is (light frequency), B is (a constant independent on the photon energy but depends on the transition probability) and $E_g$ the optical band gap. The band gap energy for all the samples may also be measured by the same method from the plot of $(\alpha h\nu)^{1/n}$ versus (hν ) energy of light, this also depended on the intersection of the tangent via inflection point in absorption band and the photon energy axis as shown in (figure - 3). Where for allowed direct transitions, n= ½, equation (3) become:

$$(\alpha h\nu)^2 = B(h\nu - E_g) \quad (5)$$

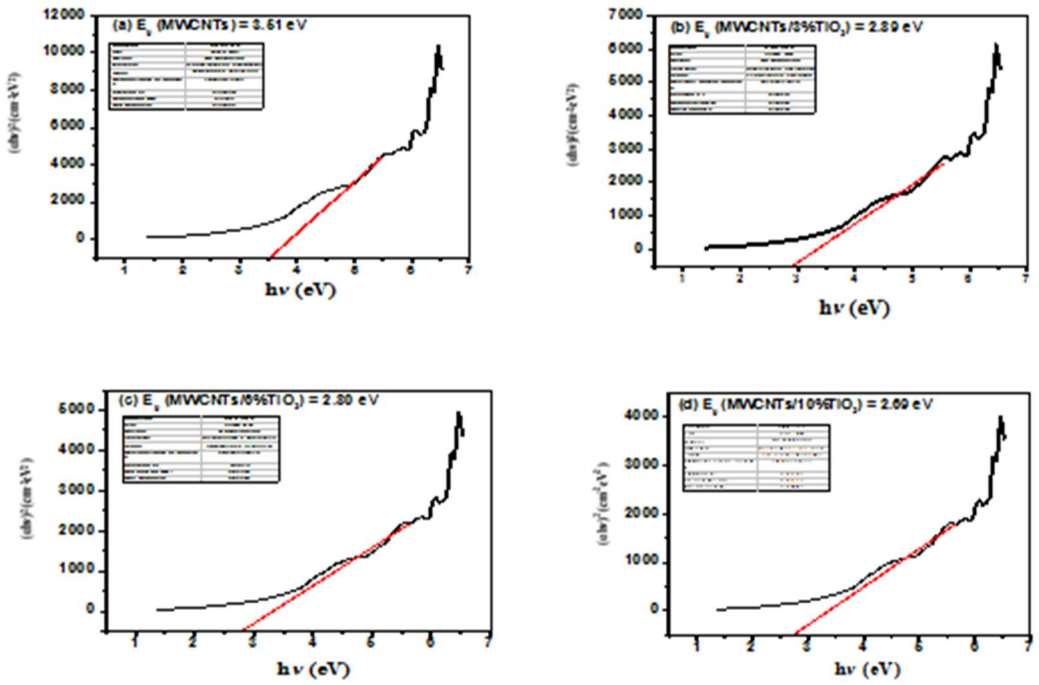


Figure 3. Kubelka-Munk curves for estimating band gap of (a) MWCNTs and (b, c and d) MWCNTs with different TiO2 % (3, 6 and 10%), respectively.

Table-1: Band gap values of MWCNTs and different MWCNTs/$TiO_2$ nanocomposites

| Photocatalyst | band gap (eV) |
|---|---|
| MWCNTs | 3.51 |
| MWCNTs/3%$TiO_2$ | 2.89 |
| MWCNTs/6%$TiO_2$ | 2.80 |
| MWCNTs/10%$TiO_2$ | 2.69 |

The optical band gap energy calculated values are shown in Table-1. The $E_g$ value of MWCNTs was 3.51 eV; it decreases to 2.89 eV for MWCNTs/3%$TiO_2$ and to 2.80 eV for MWCNTs/6%$TiO_2$ until it reaches to 2.69 eV for MWCNTs/10%$TiO_2$. This effect may be due to two reasons, an increase in vacancies or chemical defects present in the intergranular areas, also due to the chemical interaction between MWCNTs and $TiO_2$ to generate a new energy level reducing the band gap $E_g$. MWCNTs/x%$TiO_2$ nanocomposites with less band gap energy are optically active, have been extensively used in photocatalytic degradation for environmental decontamination. The decrease in band gap values suggests high photocatalytic activity of the synthesized nanocomposites in visible light range. From the obtained values, it is clear that the band gap values depend on both MWCNTs support and the $TiO_2$ percentages in the binary nanocomposites. The variation of the band gap with increasing the particle size is an important feature for photocatalytic activity of MWCNTs/x%$TiO_2$ nanocomposites [26, 27]. The interaction between MWCNTs and $TiO_2$ could be by ester bonding between carboxyl groups or by coordination of carbonyl group of MWCNTs and $TiO_2$, so the photocatalytic efficiency of the nanocomposites was enhanced.

4) *Brunauer-Emmett-Teller surface area of the synthesized MWCNTs and MWCNTs/x%$TiO_2$ nanocomposites:* Table-2 presents the surface area Brunauer-Emmett-Teller (BET) ($m^2$/g), Average pore diameter (nm), Total pore volume ($cm^3$/g) and Monolayer adsorption amount $V_m$ of the MWCNTs and MWCNTs/x%$TiO_2$ nanocomposites. The BET surface area of MWCNTs, MWCNTs/3%$TiO_2$, MWCNTs/6%$TiO_2$ and MWCNTs/10%$TiO_2$ are 95.201, 98.142, 104.251 and 117.125 $m^2$/g respectively (see Table-2 ).

Table-2: BET parameters of MWCNTs and different MWCNTs/$TiO_2$ nanocomposites

| Photocatalyst | MWCNTs | MWCNTs/3%$TiO_2$ | MWCNTs/6%$TiO_2$ | MWCNTs/10%$TiO_2$ |
|---|---|---|---|---|
| BET ($m^2$/g) | 95.201 | 98.142 | 104.251 | 117.125 |
| Total pore volume ($cm^3$/g) | 0.2139 | 0.2089 | 0.2001 | 0.1939 |
| Average pore diameter (nm) | 8.987 | 9.181 | 9.301 | 9.521 |
| $V_m$ ($cm^3$/g) | 21.843 | 22.148 | 22.800 | 23.113 |

The BET surface areas and porous structures of MWCNTs and its nanocomposites were investigated using nitrogen adsorption–desorption isotherms.

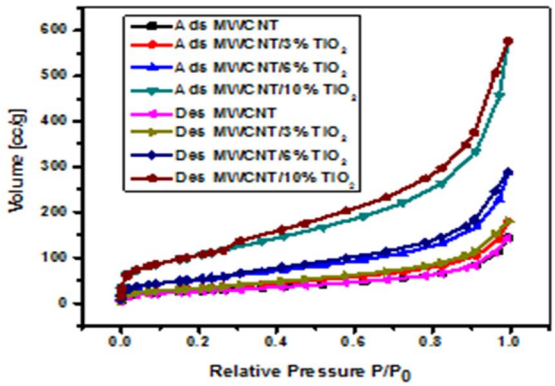


Figure - 4 displays the nitrogen adsorption-desorption for all photocatalysts.

All the photocatalysts represent type IV curves showing a typical hysteresis loop associated with capillary condensation of gases within mesopores [28]. Such mesoporous structure of photocatalysts provides efficient transport pathways to the interior, which may be useful for improving the photocatalytic activity. The smaller micro/mesopores are usually related to the primary intra-agglomeration (the hysteresis loop located in the lower $P/P_0$ range), while the larger ones are associated with secondary inter-aggregation (the hysteresis loop located in the higher $P/P_0$ range). With a further increase in the amount of $TiO_2$, however, this peak increases and broadens. This phenomenon indicates that there is a correlation between the loading of $TiO_2$ and pore size distributions of MWCNTs/x%$TiO_2$ nanocomposites. The adsorption isotherms shifts upwards and the hysteresis loop as well moves to a relatively low pressure range. From pore size distribution analysis for all samples, it observed that the smallest average pore diameter for MWCNTs which have the smallest surface area while with increasing amount of $TiO_2$ led to increase surface area because of increasing its average pore diameter as shown in Table-2. These data confirmed that the band gap decreasing in presence of $TiO_2$ and in rising its amount. This indicates that the increase of specific surface area and average pore size of the nanocomposites (Table-2) increased the photocatalytic activity of the photocatalysts that accelerated the mass transfer and generated the more reactions sites which led to the photocatalysis.

*B. Photocatalytic performance of MWCNTs and MWCNTs/x%$TiO_2$ as a photocatalysts*

1) *Study of the Effect of the Initial Dye Concentration:* The maximum absorption peaks of Dianix Blue dye and Vat Green 1 dye were located at 625 nm and 626 nm respectively. Figure - 5 (a) and (b) show that there are a positive correlation between the absorbance and the corresponding concentration of the two dye solutions. From the following figure, the suitable concentrations of the two dyes (a) and (b) used in the photodegradation processes were $2.6\times10^{-5}$ M and $2\times10^{-5}$ M respectively.

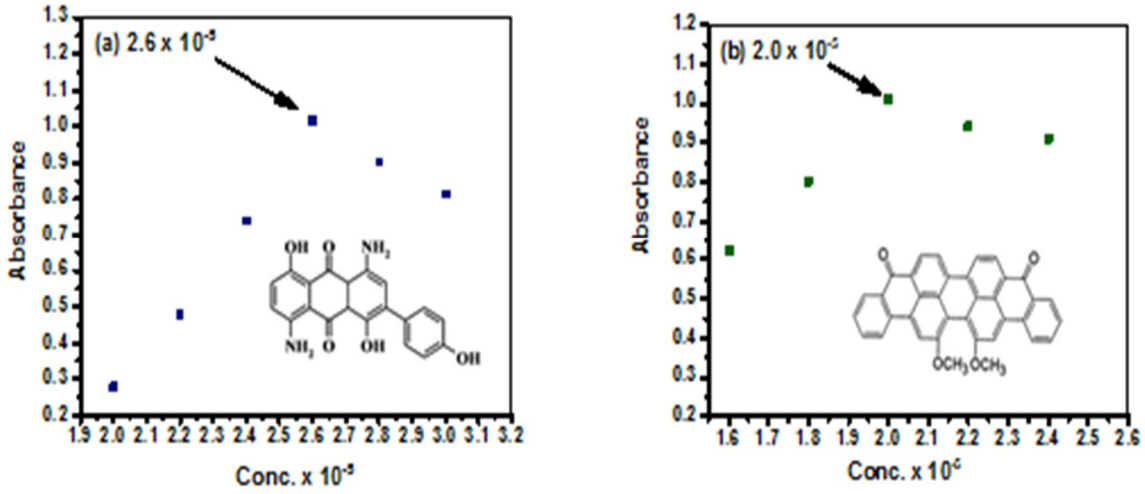


Fig.-5 Effect of concentration of Dianix Blue and Vat Green 1 dyes

2) *Photocatalytic degradation of Dianix Blue and Vat Green 1 dyes using different light sources (Sunlight, UV and Xenon irradiation).*

The photocatalytic degradation rates of the two dyes Dianix Blue and Vat Green 1 using Sunlight, UV and Xenon irradiation was monitoring spectrophotometrically in UV–Vis range as shown in Figure - 6, according to equation (6).

$$\mathrm{Ln}\ (C_0/C) = k_{app}t \qquad (6)$$

where $C_0$ is the initial concentration of the dye, C is the concentration at time t and $k_{app}$ is the apparent reaction rate constant of the photodegradation process [20]. From the Figure-6 a linear relationships were obtained between ln ($C_0$/C) and irradiation time. The photocatalytic experiments of the two dyes follow the pseudo first order kinetics. Three sets of experiments for each dye were performed using three types of light sources (Sunlight, UV and Xenon) respectively in presence of MWCNTs and MWCNTs/x%$TiO_2$ nanocomposites (where x=3, 6 and 10) to observe the adsorption and photocatalytic effects of MWCNTs on the synthesized nanocomposites, the BET surface area of MWCNTs and MWCNTs/3%$TiO_2$, MWCNTs/6%$TiO_2$,MWCNTs/10%$TiO_2$ are 95.201, 98.142, 104.251 and 117.125 $m^2/g$ respectively (see Table-2 ). There is rapid recombination between conduction band

electrons and valence band holes in $TiO_2$ photocatalyst. However, after introducing the MWCNTs in the synthesized MWCNTs/x%$TiO_2$ nanocomposites, the photocatalytic activity was enhanced and increased, this can be attributed to the synergetic effects of adsorption on multi walled carbon nanotubes in MWCNTs/x%$TiO_2$ nanocomposites. This enhancement in photocatalytic activity of the nanocomposites supports the idea of formation of a common contact interface between the multi walled carbon nanotubes and $TiO_2$ in the nanocomposite, where MWCNTs acts as an efficient adsorption trap of the two dyes, this led to rapid photocatalytic degradation.

The slopes which represent the photocatalytic reaction rate constants ($k_{app}$) and the synergy factors (R) were calculated, the products of the photodegradation processes using Chemical Oxygen Demand (COD) values were measured, all values are listed in Table-3. Comparing the $k_{app}$ for all photodegradation processes of the dyes using MWCNTs, MWCNTs/3%$TiO_2$, MWCNTs/6%$TiO_2$, MWCNTs/10%$TiO_2$ photocatalysts, The photodegradation rate increases greatly in the existence of MWCNTs and in the order of MWCNTs-MWCNTs/3%$TiO_2$-MWCNTs/6%$TiO_2$-MWCNTs/10%$TiO_2$ respectively, where The BET surface area of MWCNTs and MWCNTs/3%$TiO_2$, MWCNTs/6%$TiO_2$, MWCNTs/10%$TiO_2$ are 95.201, 98.142, 104.251 and 117.125 $m^2/g$ respectively (see Table-2) and depending on the $TiO_2$ percent in the nanocomposites, where increasing of the photogenerated charge carriers (electron-hole pair) led to high photocatalytic e□ciency. As expected when $TiO_2$ is exposed to photons and the electrons are transfer from the valence band (VB) to the conduction band (CB) resulting in the formation of equal numbers of holes in the valence band, as in (equation 7).

$$TiO_2 + h\nu \rightarrow h^+ + e^- \quad (7)$$

The electrons in the CB react with $O_2$ to yield superoxide anion radicals $O_2^{\cdot -}$ that oxidize the two dyes under investigation according to (equation 8).

$$e^- + O_2 \rightarrow O_2^{\cdot -} \quad (8)$$

On the other hand, the adsorbed water or hydroxyl anions were reacted with the holes of the VB to produce hydroxyl radicals as in equations (9) and (10).

$$H_2O + h^+ \rightarrow H^+ + {}^{\cdot}OH \quad (9)$$

$$OH^- + h^+ \rightarrow {}^{\cdot}OH \quad (10)$$

The generated hydroxyl radicals attack the organic dyes adsorbed onto the photocatalyst surface in solution and oxidized them [29, 30]. The hydroxyl radical which produced from the oxidation of adsorbed water or $OH^-$ during the degradation of the organic dyes is considered as the primary oxidant; as well dissolved oxygen in solution alter the recombination of ($h^+$- $e^-$ pairs). From the results of MWCNTs exist in the prepared nanocomposites, causing an increase in the decolourization rate as shown in Figure-6, multi-walled carbon nanotubes MWCNTs with excellent adsorption capacity enhance the lifetime of the separated charge carriers, hindering (electron $e^-$ - hole $h^+$ pair) recombination of the synthesized nanocomposites more than $TiO_2$ alone and provide an increase in synergistic effect in all photodegradation processes of the dyes using nanocomposites than $TiO_2$. The possible role of MWCNTs in the prepared nanocomposites on the photocatalytic processes could be investigated due to the generation of electrons ($e^-$) by different light sources which transferred to conduction band of $TiO_2$ (MWCNTs act as electron source), in the same time the electrons of $TiO_2$ were transferred to MWCNTs (MWCNTs act as electron sink) simultaneously. In other hand, the holes ($h^+$) generated during the induced electrons migrated from MWCNTs to $TiO_2$. The transferred electrons ($e^-$) from MWCNTs to $TiO_2$ could react with the $O_2$ adsorbed on the surface of $TiO_2$ to produce very active superoxide anion radicals. The produced superoxide radical ions, the positive charged holes ($h^+$) could react with $OH^-$ or adsorbed $H_2O$ to produce hydroxyl radicals. The produced superoxide radical ions $O_2^{\cdot -}$ and hydroxyl radicals ${}^{\cdot}OH$ were responsible for the photodegradation of the dyes. The dominant contribution of MWCNTs in MWCNTs/x%$TiO_2$ nanocomposites is mainly determined by an increase in recombination time for photogenerated $h^+$- $e^-$ pairs. MWCNTs can act as an electron sink leading to ($h^+$- $e^-$ separation) because of its delocalized π-electronic structure that facilitates the transfer of photogenerated electrons as shown in Figure-7. The injected electrons are transferred to the oxygen $O_2$ to generate the highly active superoxide anion radical $O_2^{\cdot -}$, helping the photodegradation process of the dyes adsorbed on MWCNTs surface. Also, due to the interphase interactions between $TiO_2$ and MWCNTs in the synthesized MWCNTs/x%$TiO_2$ nanocomposites, the photocatalytic activity of the nanocomposites were improved.

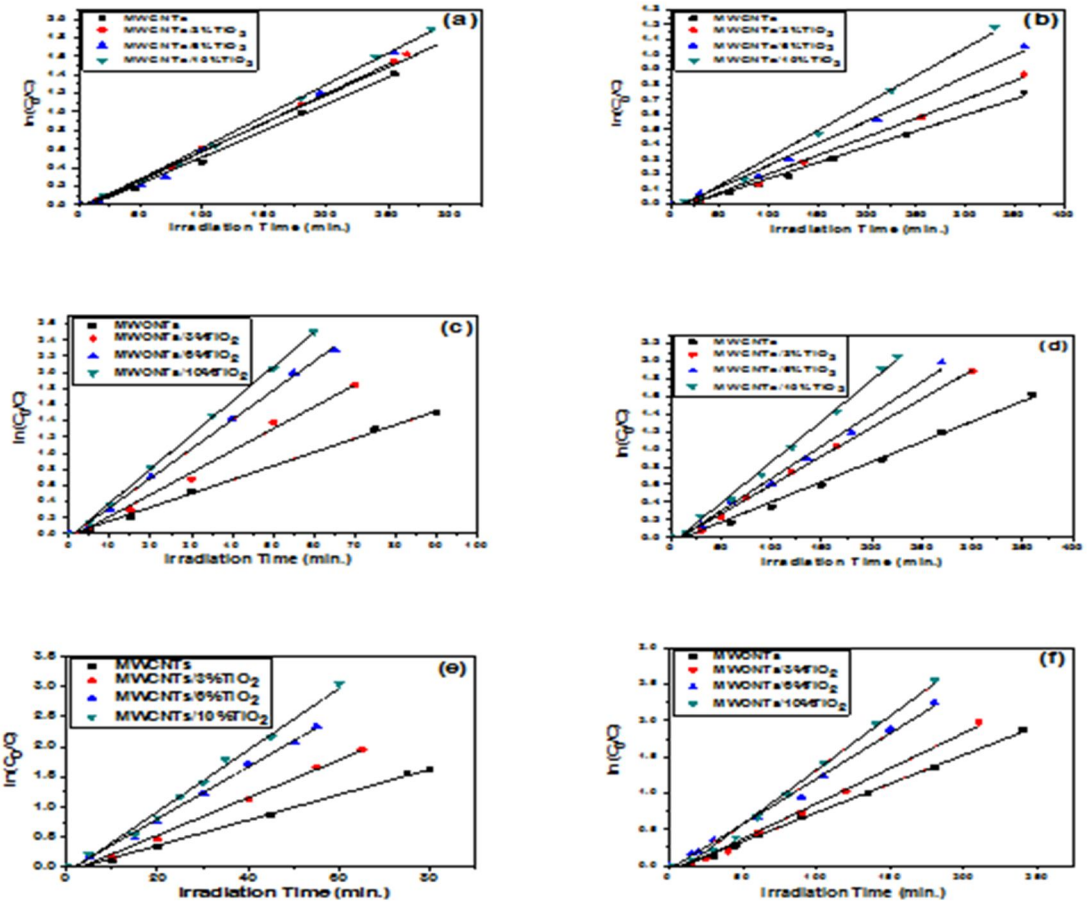


Figure-6 shows pseudo first order linear plots of ln ($C_0$/C) vs. irradiation time for the degradation kinetics of Dianix Blue dye (a, c and e) and Vat Green 1 dye (b, d and f) under different Sunlight, UV and Xenon irradiation, respectively.

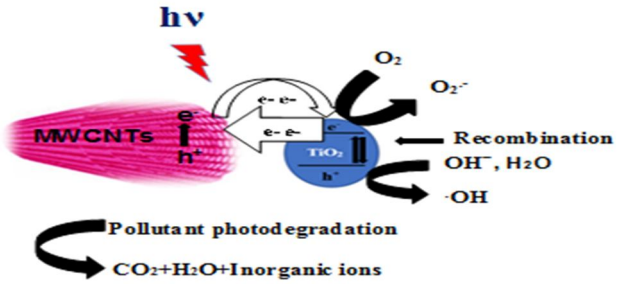


Figure-7 shows schematic diagram of the proposed mechanism of photocatalytic degradation over MWCNTs /$TiO_2$ nanocomposite.

*3) The synergy factor (R) of MWCNTs:* The synergy factor (R) is expressed as in equation (11).

$$R = \left(\frac{kapp(MWCNTs/x\%TiO2)}{kapp(MWCNTs)}\right) \quad (11)$$

Where $k_{app}$(MWCNTs/x%$TiO_2$), $k_{app}$(MWCNTs) refers to the apparent rate constant for the photocatalytic activity in the existence of the nanocomposite and MWCNTs respectively [20, 27]. The photocatalytic activity of the dyes depends on the adsorption on the surface of photocatalysts. Table-3 shows photodegradation rates ($k_{app}$), synergy factors (R) and Chemical Oxygen Demand (COD) of the two dyes with MWCNTs and MWCNTs/3%$TiO_2$, MWCNTs/6%$TiO_2$, MWCNTs/10%$TiO_2$ nanocomposites in the existence of Sunlight, UV and Xenon irradiation respectively.

Generally, the organic pollutant dyes can't degraded completely under Sunlight irradiation and according to Egyptian Environmental Law (Law NO.9), The COD value allowed is less than 1000 ppm [31, 32]. From the above table, the photodegradation of the two

dyes under Sunlight in presence of MWCNTs and MWCNTs/x%$TiO_2$ nanocomposites still had COD (ppm) values higher than the allowed value (1000 ppm). While the photodegradation of the two dyes on the MWCNTs/x%$TiO_2$ nanocomposites surfaces exposed to both of UV and Xenon light sources recorded COD values less than 1000 (ppm), especially the MWCNTs/10%$TiO_2$ samples which has COD values less than 1000 (ppm), this indicate that they are used as excellent photocatalysts. It can be seen from Table-3 that the photocatalytic degradation process of the dyes increases with increasing the $TiO_2$ weight percent in the nanocomposites from 3 to 10% and reaches its maximum at a 10%$TiO_2$ in the nanocomposite. Also the highest photodegradation rate was observed using Xenon irradiation with MWCNTs/10%$TiO_2$ nanocomposite, where the number of dye molecules adsorbed on the photocatalysts and the number of photons absorbed were increased which promotes the photodegradation rate.

Table-3: Photodegradation rates ($k_{app}$), synergy factors (R) and Chemical Oxygen Demand (COD) values of the two dyes with different photocatalysts in the existence of different irradiation sources.

| | | | | |
|---|---|---|---|---|
| Sunlight irradiation | Dianix Blue dye | | | |
| | Photocatalyst | $k_{app}$ ($s^{-1}$) | R | COD (ppm) |
| | MWCNTs | 0.00571 ± 1.95619E-4 | 1 | 2645 |
| | MWCNTs/3%$TiO_2$ | 0.00622 ± 9.45456E-5 | 1.089 | 2470 |
| | MWCNTs/6%$TiO_2$ | 0.00658 ± 2.44397E-4 | 1.152 | 2108 |
| | MWCNTs/10%$TiO_2$ | 0.00679 ± 1.52953E-4 | 1.189 | 1985 |
| | Vat Green 1 dye | | | |
| | Photocatalyst | $k_{app}$ ($s^{-1}$) | R | COD (ppm) |
| | MWCNTs | 0.00212 ± 7.95952E-5 | 1 | 3785 |
| | MWCNTs/3%$TiO_2$ | 0.00248 ± 1.03928E-4 | 1.169 | 3205 |
| | MWCNTs/6%$TiO_2$ | 0.00294 ± 1.11411E-4 | 1.386 | 2988 |
| | MWCNTs/10%$TiO_2$ | 0.00366 ± 1.36129E-4 | 1.726 | 2645 |
| UV irradiation | Dianix Blue dye | | | |
| | Photocatalyst | $k_{app}$ ($s^{-1}$) | R | COD ( ppm ) |
| | MWCNTs | 0.017 ± 3.50919E-4 | 1 | 2258 |
| | MWCNTs/3%$TiO_2$ | 0.02711 ± 0.00111 | 1.594 | 1310 |
| | MWCNTs/6%$TiO_2$ | 0.03612 ± 5.76817E-4 | 2.124 | 1025 |
| | MWCNTs/10%$TiO_2$ | 0.04213 ± 5.54871E-4 | 2.478 | 865 |
| | Vat Green 1 dye | | | |
| | Photocatalyst | $k_{app}$ ($s^{-1}$) | R | COD ( ppm ) |
| | MWCNTs | 0.00458 ± 1.21127E-4 | 1 | 2185 |
| | MWCNTs/3%$TiO_2$ | 0.00653 ± 1.52995E-4 | 1.425 | 1764 |
| | MWCNTs/6%$TiO_2$ | 0.00732 ± 2.23643E-4 | 1.598 | 1388 |
| | MWCNTs/10%$TiO_2$ | 0.00929 ± 1.99737E-4 | 2.028 | 925 |
| Xenon irradiation | Dianix Blue dye | | | |
| | Photocatalyst | $k_{app}$ ($s^{-1}$) | R | COD ( ppm ) |
| | MWCNTs | 0.02114 ± 5.88147E-4 | 1 | 2101 |
| | MWCNTs/3%$TiO_2$ | 0.03128 ± 0.00119 | 1.479 | 1156 |
| | MWCNTs/6%$TiO_2$ | 0.04332 ± 0.00114 | 2.049 | 864 |
| | MWCNTs/10%$TiO_2$ | 0.05126 ± 0.00168 | 2.424 | 714 |
| | Vat Green 1 dye | | | |
| | Photocatalyst | $k_{app}$ ($s^{-1}$) | R | COD ( ppm ) |
| | MWCNTs | 0.00795 ± 1.53579E-4 | 1 | 1785 |
| | MWCNTs/3%$TiO_2$ | 0.00973 ± 3.45827E-4 | 1.223 | 1325 |
| | MWCNTs/6%$TiO_2$ | 0.01251 ± 3.55707E-4 | 1.573 | 1080 |
| | MWCNTs/10%$TiO_2$ | 0.01491 ± 5.29326E-4 | 1.875 | 897 |

## IV. CONCLUSION

Semiconductor photocatalysis seems to be a promising technology that encompasses a range of applications in environmental systems such as hazardous waste remediation, air purification. Photocatalytic oxidation using MWCNTs and MWCNTs/3%$TiO_2$, MWCNTs/6%$TiO_2$, MWCNTs/10%$TiO_2$ nanocomposites in the presence of Sunlight, UV and Xenon lights were effectively applied for the photodegradation of Dianix Blue and Vat Green 1 dyes. It can be deduced that the synergistic effect of MWCNTs, the percentage of $TiO_2$ in nanocomposites, polymorphs of $TiO_2$ due to the dominant structure which cause high levels of crystalline of the nanocomposites, and the synthesis method of the nanocomposites, all affect the photodegradation processes significantly. According to these results, it could be suggested that the nanocomposites had a good photocatalytic effectiveness especially the samples MWCNTs/10%$TiO_2$. Both of the photodegradation rates k ($s^{-1}$) and the synergy factors (R) were increased, also the photodegradation processes using COD analysis revealed a higher degree of complete mineralization of the two textile dyes especially by using Xenon irradiation, so these nanocomposites were an effective for the removal of the dyes from aqueous solutions and follow COD limits of Egyptian Environmental Law (Law NO.9).

## REFERENCES

[1] A. M. Kamil, H. T. Mohammed, A. A. Balakit, F. H. Hussein, D. W. Bahnemann, and G. A. El-Hiti, "Synthesis, Characterization and Photocatalytic Activity of Carbon Nanotube/Titanium Dioxide Nanocomposites" Arab. J. Sci. Eng., vol. 43, No. 1, pp. 199-210, 2018.
[2] Y. Huang, R. Li, D. Chen, X. Hu, P. Chen, Z. Chen, and D. Li, "Synthesis and Characterization of CNT/$TiO_2$/ZnO Composites with High Photocatalytic Performance" Catalysts, vol. 8, No. 4, pp. 151-156, 2018.
[3] J. O. Marques Neto, C. R. Bellato, C. H. F. De Souza, R. C. Da Silva, and P. A. Rocha, "Synthesis, Characterization and Enhanced Photocatalytic Activity of Iron Oxide/Carbon Nanotube/Ag-doped $TiO_2$ Nanocomposites"J. Braz. Chem. Soc., vol. 28, No. 12, pp. 2301-2312 ,2017.
[4] N. M. Mahmoodi, P. Rezaei, C. Ghotbei, and M. Kazemeini, Fibers, "Copper oxide-carbon nanotube (CuO/CNT) nanocomposite: Synthesis and photocatalytic dye degradation from colored textile wastewater" Polym., vol. 17, No. 11, pp. 1842-1848 , 2016.
[5] M. Shaban, A. M. Ashraf, and M. R. Abukhadra, "TiO2 Nanoribbons/Carbon Nanotubes Composite with Enhanced Photocatalytic Activity; Fabrication, Characterization, and Application" Characterization, and Application. Sci. Rep., vol. 8, No. 781, 1-17, 2018.
[6] A. Salama, A. Mohamed, N. M. Aboamera, T. A. Osman, and A. Khattab, "Photocatalytic degradation of organic dyes using composite nanofibers under UV irradiation"Appl. Nanosci., vol. 8, pp. 155-161 , 2018.
[7] A. Mohamed, S. Yousef, M. Ali Abdelnaby, T.A. Osman, B. Hamawandi, M.S. Topark, M. Muhammed and A. Uheida, "Photocatalytic degradation of organic dyes and enhanced mechanical properties of PAN/CNTs composite nanofibers"Sep. Purif. Technol., vol. 182, pp. 219-223, 2017.
[8] W. Zhu, Z. Li, C. He, S. Faqian and Y. Zhou, "Enhanced photodegradation of sulfamethoxazole by a novel $WO_3$-CNT composite under visible light irradiation" J. Alloys Compd., vol. 754, pp. 153-162, 2018.
[9] R. S. Lankone, J. Wang, J. F. Ranville, and D. H. Fairbrother, "Photodegradation of polymer-CNT nanocomposites: effect of CNT loading and CNT release characteristics"Environmental Science: Nano, vol. 4, 967-982, 2017.
[10] W. Yang, L. Lang, X. Yin, and C. Wu, "Formation mechanism of 0.4-nm single-walled carbon nanotubes in $AlPO_4$-5 crystals by low-temperature hydrocracking" Carbon, vol. 115, pp. 120-127, 2017.
[11] D. Eder, "Carbon Nanotube−Inorganic Hybrids" Chem. Rev., vol. 110, pp. 1348-1385, 2010.
[12] J. Moma, J. Baloyi, and T. Ntho, "Synthesis and characterization of an efficient and stable Al/Fe pillared clay catalyst for the catalytic wet air oxidation of phenol"RSC Adv., vol. 8, pp. 30115-30124, 2018.
[13] M. Loginov, N. Lebovka, and E. Vorobiev, "Hybrid Multiwalled Carbon Nanotube − Laponite Sorbent for Removal of Methylene Blue from Aqueous Solutions" Journal of Colloid and Interface Science, vol. 431, pp. 241-249, 2014.
[14] D. M. El-Mekkawi, A. A. Labib, H. A. Mousa, H. R. Galal, and W. A. A. Mohamed, "Preparation and Characterization of Nano Titanium Dioxide Photocatalysts Via Sol Gel Method over Narrow Ranges of Varying Parameters" Orient. J. Chem., vol. 33, No. 1, pp. 41-51, 2017.
[15] A. Aliyu, A. Abdulkareem, A. Kovo, O. Abubakre, J. Tijani, and I. Kariim, "Synthesize multi-walled carbon nanotubes via catalytic chemical vapour deposition method on Fe-Ni bimetallic catalyst supported on kaolin" Carbon Letters, vol. 21, No. 33, pp. 33-50, 2017.
[16] G. Ma, Y. Zhu, Z. Zhang, and L. Li, "Preparation and characterization of multi-walled carbon nanotube/TiO"2 composites: Decontamination organic pollutant in water" Appl. Surf. Sci., vol. 313, pp. 817-822, 2014.
[17] A. M. Kamil, F. H. Hussein, A. F. Halbus, and D. W. Bahnemann, "Preparation, Characterization, and Photocatalytic Applications of MWCNTs/$TiO_2$ Composite" International Journal of Photoenergy, vol. 2014, No. 1, pp. 1-8, 2014.
[18] I. Ali, M. Suhail, Z. A. Alothman, and A. Alwarthan, "Recent advances in syntheses, properties and applications of $TiO_2$ nanostructures" RSC Adv., vol. 8, pp. 30125-30147, 2018.
[19] D. Heltina, P. P. D. K. Wulan, and Slamet, "Synthesis and Characterization of Titania Nanotube-Carbon Nanotube Composite for Degradation of Phenol" Journal of Chemical Engineering, vol. 6, pp. 1065-1068, 2015.
[20] G. Rahman, Z. Najaf, A. Mehmood, S. Bilal, A. Shah, S. Mian, and G. Ali, "An Overview of the Recent Progress in the Synthesis and Applications of Carbon Nanotubes" Journal of Carbon Research, vol. 5, No. 1, pp. 1-31, 2019.
[21] G. Allaedini, S. M. Tasirin, and P. Aminayi, "Synthesis of CNTs via chemical vapor deposition of carbon dioxide as a carbon source in the presence of NiMgO" Journal of Alloys and Compounds, vol. 647, pp. 809-814, 2015.
[22] C. E. El shafiee, M. O. Abdel-salam, S. M. N. Moalla , H. R. Ali , D. I. Osman, R. I. Abdallah , and Y.M. Moustafa, "Carbon Nanotubes as Superior Sorbent for Removal of Phenol from Industrial Waste Water" Egy. J. Chem., vol. 61, No. 1, pp. 75-84, 2018.
[23] A. Alwash, H. Adil, Z. Hussain, and E. Yousif, "Potential of Carbon Nanotubes in Enhance of Photocatalyst Activity" Arch. Nanomedicine, vol. 1, No. 3, pp. 65-70, 2018.

[24] A. A. Ismail, A. M. Ali, F. A. Harraz, M. Faisal, H. Shoukry, and A. E. Al-Salami, "A Facile Synthesis of alpha-Fe2O3/Carbon Nanotubes and Their Photocatalytic and Electrochemical Sensing Performances" Int. J. Electrochem. Sci., vol. 14, pp. 15-32, 2019.
[25] M. Nowak, B. Kauch and P. Szperlich, "Determination of energy band gap of nanocrystalline SbSI using diffuse reflectance spectroscopy" Rev. Sci. Instrum., vol. 80, No. 4, pp. 1- 12, 2009.
[26] M. Chandrakala, S. Raj Bharath, T. Maiyalagan and S. Arockiasamy, "Synthesis, crystal structure and vapour pressure studies of novel nickel complex as precursor for NiO coating by metalorganic chemical vapour deposition technique" Mater. Chem. Phys., vol. 201, pp. 344-353, 2017.
[27] M. Thirumoorthi and J. T. J. Prakash, "Effect on the properties of ITO thin films in Gamma environment" J. Superlattices and Microstructures, vol. 85, pp. 237-247, 2015.
[28] J. Yu, T. Ma, G. Liu and B. Cheng, "Enhanced photocatalytic activity of bimodal mesoporous titania powders by $C_{60}$ modification" Dalt. Trans., vol. 40, pp. 6635-6644, 2011.
[29] J. G. Yu, X. H. Zhao, H. Yang, X. H. Chen, Q. Yang, L. Y. Yu, J. H. Jiang, and X. Q. Chen, "Aqueous adsorption and removal of organic contaminants by carbon nanotubes" Science of the Total Environment, vol. 482, pp. 241-251, 2014.
[30] E. F. A. Zeid, I. A. Ibrahem, A. M. Ali, and W. A. A. Mohamed, "The effect of CdO content on the crystal structure, surface morphology, optical properties and photocatalytic efficiency of p-NiO/n-CdOnanocomposite" Results Phys., vol. 12, pp. 562-570, (2019).
[31] U.S. Environmental Protection Agency (EPA). (2008) EPA's 2008 Report on the Environment. National Center for Environmental Assessment, Washington, DC; EPA/600/R-07/045F, http://www.epa.gov/roe, 2008.
[32] Affairs, E., Law Number 9 of 2009 on Investment. http://www.eeaa.gov.eg/en-us/laws/envlaw.aspx, 2009.

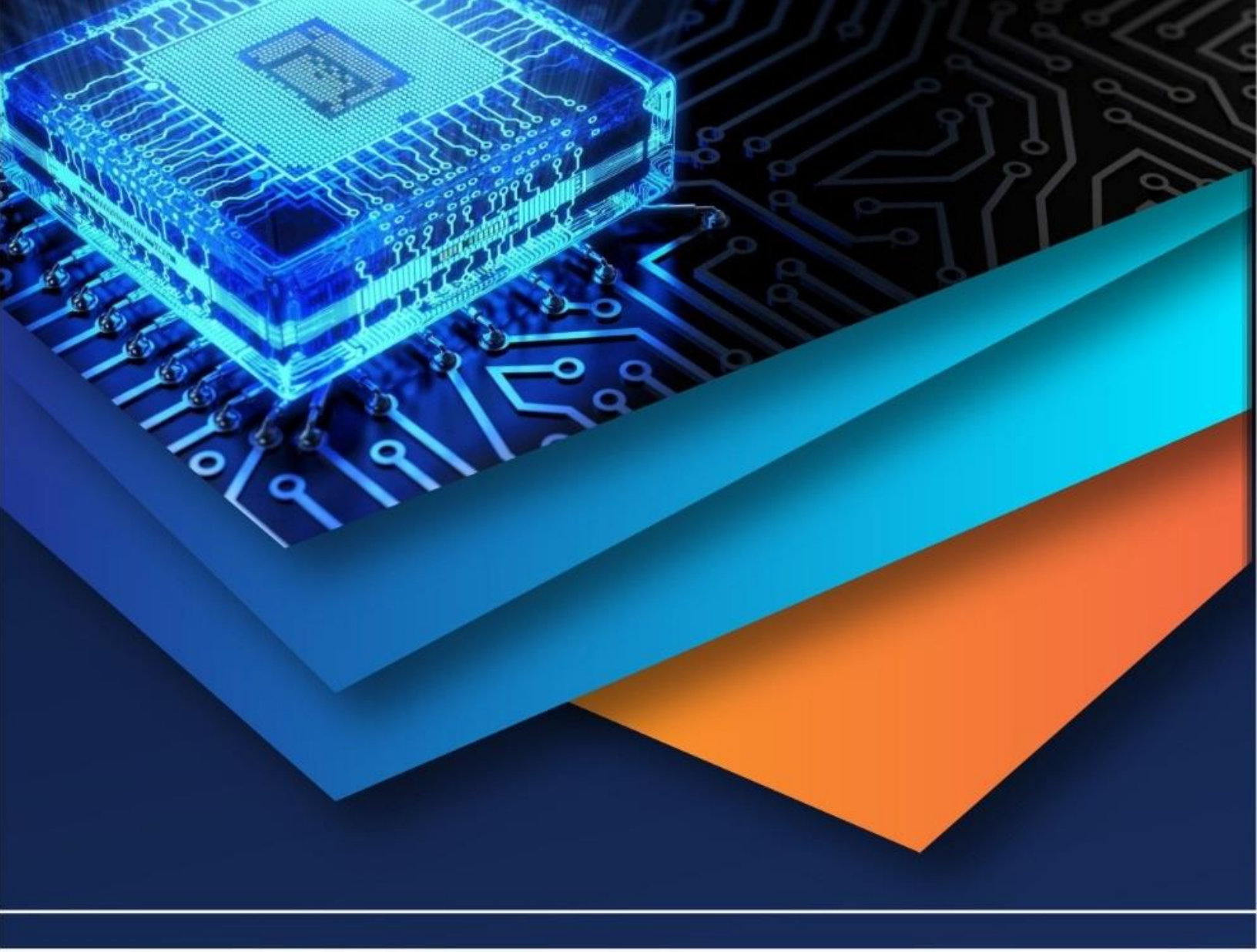

10.22214/IJRASET

45.98

IMPACT FACTOR: 7.129

IMPACT FACTOR: 7.429

# INTERNATIONAL JOURNAL FOR RESEARCH

IN APPLIED SCIENCE & ENGINEERING TECHNOLOGY